

Hybrid conjugated polymer solar cells using patterned GaAs nanopillars

Giacomo Mariani,^{1,a)} Ramesh B. Laghumavarapu,¹ Bertrand Tremolet de Villers,² Joshua Shapiro,¹ Pradeep Senanayake,¹ Andrew Lin,¹ Benjamin J. Schwartz,^{2,3} and Diana L. Huffaker^{1,3}

¹Department of Electrical Engineering, University of California at Los Angeles, Los Angeles, California 90095, USA

²Department of Chemistry and Biochemistry, University of California at Los Angeles, Los Angeles, California 90095, USA

³California NanoSystems Institute, University of California at Los Angeles, Los Angeles, California 90095, USA

(Received 28 April 2010; accepted 9 June 2010; published online 9 July 2010)

In this work, we study hybrid solar cells based on poly(3-hexylthiophene)-coated GaAs nanopillars grown on a patterned GaAs substrate using selective-area metal organic chemical vapor deposition. The hybrid solar cells show extremely low leakage currents ($I \cong 45$ nA @ -1 V) under dark conditions and an open circuit voltage, short circuit current density, and fill factor of 0.2 V, 8.7 mA/cm², and 32%, respectively, giving a power conversion efficiency of $\eta=0.6\%$ under AM 1.5 G illumination. Surface passivation of the GaAs results in further improvement, yielding $\eta=1.44\%$ under AM 1.5 G illumination. External quantum efficiency measurements of these polymer/inorganic solar cells are also presented. © 2010 American Institute of Physics. [doi:10.1063/1.3459961]

In the past few years polymer solar cells have gained attention due to their low cost, flexibility and ease of manufacturing.¹ Although conjugated polymers benefit from high absorption coefficients compared to inorganic semiconductors, low carrier mobilities ($\sim 10^{-4}$ cm² V⁻¹ s⁻¹) limit their energy conversion efficiency to less than 8%.² In contrast, inorganic solar cells have high carrier mobilities, enabling effective charge extraction and thus high quantum efficiencies. This suggests exciting possibilities for hybrid polymer/inorganic solar cells, which may be designed to simultaneously exploit the high carrier mobility from inorganic semiconductors and strong absorption coefficient from the polymer. Such a hybrid approach could effectively remove the carrier transport bottleneck suffered in conjugated polymers through the use of integrated III–V inorganic nanostructures.

Much of the recent work in hybrid photovoltaics has aimed to augment the power conversion efficiency by embedding silicon nanocrystals,³ or nanorods⁴ and quantum dots⁵ of II–VI inorganic semiconductors into a semiconducting polymer matrix. Surprisingly, relatively little work has been done involving hybrid solar cells with III–V inorganic nanostructures, despite the high efficiencies achieved in III–V bulk solar cells. The only report of a hybrid photovoltaic device involving III–V materials that we are aware of takes advantage of *n*-doped GaAs nanowires (via Au-catalyst growth) in combination with poly(3-hexylthiophene) (P3HT) and has shown an energy conversion efficiency of 1.04%.⁶

In this paper, we present a type of hybrid inorganic/conjugated polymer photovoltaic device based on an array of patterned P3HT-coated *n*-GaAs nanopillar heterojunctions, shown in Fig. 1. By using patterned growth rather than catalyzed, we create a highly crystalline material free from residual Au-dopants, which results in very low leakage current.⁷ Moreover, the highly regular geometric structure

increases the optical path length by several times due to confinement of the optical rays in the nanostructured array, thereby enhancing the optical absorbance with respect to the bulk counterpart.⁸

The *n*-doped GaAs nanopillars are grown by selective-area metal organic chemical vapor deposition (MOCVD) using a 300 Å SiO₂ mask evaporated onto a GaAs (111)B *n*⁺-doped substrate. Multiple 1 cm² dies are patterned by e-beam lithography with 500 × 500 μm² patches on a 600 nm pitch. Trimethyl-gallium and tertiary-butyl-arsine source gases are flowed for 60 min with a V/III flux ratio of 8.5 and equivalent planar growth rate of 0.5 Å/s. Disilane is introduced to dope the pillars with a nominal doping concentration of 7 × 10¹⁸ cm⁻³ from previous thin-film calibrations.

Prior to any processing step, the samples are characterized by scanning electron microscopy (SEM), as shown in Fig. 2(a). The average nanopillar diameter and height are about 250 nm and 1.3 μm, respectively. An annealed AuGe/Ni/Au alloy forms the bottom ohmic contact. Prior to the polymer spin-coating, the samples are chemically treated in aqueous HCl (10 v/v%) solution at room temperature for 30 s to remove any native oxide on the pillar surface that

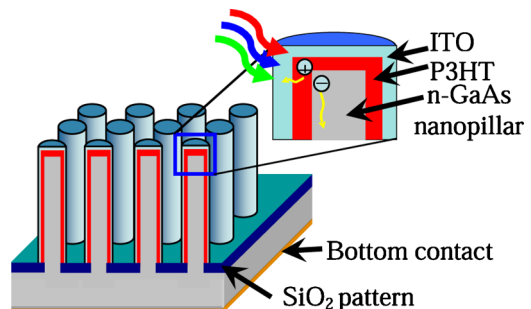


FIG. 1. (Color online) Schematic diagram of the GaAs/P3HT hybrid solar cell.

^{a)}Electronic mail: giacomomariani@ucla.edu.

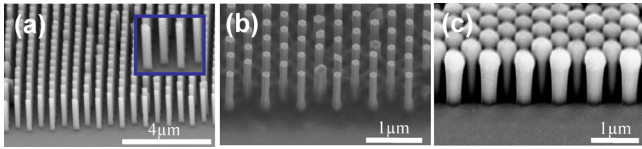


FIG. 2. (Color online) Cross-Sectional SEM of (a) an array of patterned *n*-doped GaAs nanopillars grown by MOCVD, (b) nanopillar array after P3HT spin-coating, and (c) final hybrid device with ITO top contact.

could hinder the carrier extraction at the interface of the junction.

The hybrid solar cells are prepared by spin-coating regioregular P3HT (P3HT; 90%–93%, Rieke Metals) from an *o*-dichlorobenzene solution onto the nanopillar samples to produce a polymer film thickness of about 100 nm (as measured on flat substrate). The SEM image in Fig. 2(b) shows that P3HT clings uniformly to the base and sides of the pillars, with only a thin layer on top. To complete the devices, transparent indium tin oxide ($\text{SnO}_2/\text{In}_2\text{O}_3$ 10:90 wt %) (ITO) is rf sputtered at room temperature, providing an anode with an optical transmittance greater than 85% (for $400 \text{ nm} < \lambda < 1000 \text{ nm}$) and a sheet resistance of $20 \ \Omega/\square$ (from planar calibrations). Figure 2(c) shows that the sputtered ITO completely covers the nanopillars, forming a ball on top of each pillar. We also fabricated control devices with the same nanopillar growth, bottom contact and ITO as a transparent front electrode, without any P3HT deposition, as well as control devices with P3HT spun on to the patterned- SnO_2 covered GaAs substrate without nanopillars. We performed photoluminescence (PL) measurements on all of our devices and found complete PL quenching for the devices with nanopillars and no PL quenching for the control devices without nanopillars. Figure 3 shows the J-V characteristics of the P3HT/GaAs hybrid solar cell, measured both in the dark and under AM 1.5 G (1 sun) illumination (1000 W m^{-2}). The active device area is 0.25 mm^2 and encompasses approximately 250 000 nanopillars.

The device exhibits an open circuit voltage (V_{OC}) of 0.2 V, a short circuit current (I_{SC}) of 8.7 mA/cm^2 , and fill factor (FF) of 32%. The measured power conversion efficiency is $\eta=0.6\%$. Under dark conditions, these devices exhibit very low leakage currents ($I_{\text{LEAKAGE}}=110 \text{ nA @ -1V}$), which we attribute to extremely high crystallinity of the

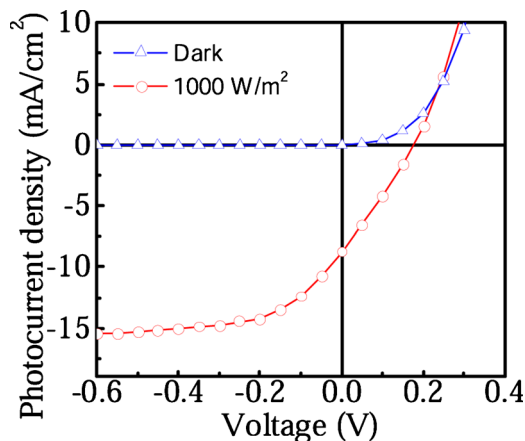


FIG. 3. (Color online) Current-voltage characteristics of the hybrid solar cell using P3HT and as-grown GaAs nanopillars (without ammonium sulfide passivation) under both dark conditions and AM 1.5 G (1 sun) illumination.

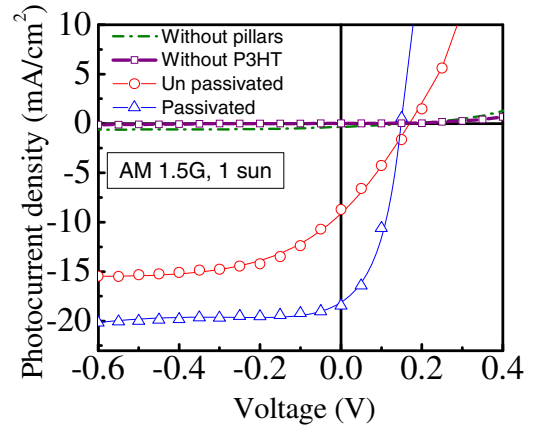


FIG. 4. (Color online) Comparison of current-voltage characteristics of the passivated and unpassivated hybrid solar cells along with a control cell without P3HT and another one without pillars. Measurements are done under AM 1.5 G (1 sun) illuminations.

GaAs nanopillars and the high quality of the pillar/substrate interface quality. Furthermore, since the patterned nanopillars are grown catalyst free, they contain no residual dopants from catalyst material such as Au.⁹

The overall performance of the hybrid solar cells demonstrated here are likely limited by several factors. The offset of the GaAs conduction band and the P3HT lowest unoccupied molecular orbital is large; although this helps encourage electrons from P3HT excitons to transfer into the GaAs conduction band, it also likely results in the observed low V_{OC} . Second, the presence of surface states on the GaAs nanopillars, caused by dangling bonds on the nanopillar surface or by residual native oxide, are known to introduce nonradiative recombination sites, trap charges,¹⁰ and pin the Fermi level to midgap. These effects can alter the effective doping concentration and deplete the nanopillars, reducing the size of their conducting channels.¹¹

Fortunately, it is known that chemical passivation can reduce both surface state density and surface recombination velocity.¹² Both theoretical¹³ and experimental¹⁴ analyses suggest that ammonium sulfide represents a suitable surface passivation agent, enhancing optical performance and eliminating the surface states on the nanopillar facets. Thus, we prepared a second set of hybrid devices in which the GaAs nanopillars were passivated in aqueous ammonium sulfide [$(\text{NH}_4)_2\text{S}$] solution (22 v/v%) for 60 min at room temperature to minimize the surface-state density. We found an equal extent of PL quenching for the passivated and nonpassivated samples, indicating that the passivation step did not significantly affect exciton harvesting. Figure 4 compares the J-V characteristics of the hybrid cells with and without surface passivation (as well as the control cells without either any P3HT or any nanopillars). The samples that underwent passivation treatment exhibited a noticeable improvement in overall performance; despite a small reduction in V_{OC} (from 0.2 to 0.18 V), I_{SC} increases from 8.7 to 18.6 mA/cm^2 and the FF improves from 32% to 43%, resulting in a power conversion efficiency of $\eta=1.44\%$ with leakage current $I_{\text{LEAKAGE}}=45 \text{ nA @ -1V}$ (under dark conditions).

Figure 5 shows the external quantum efficiency (EQE) data for passivated and unpassivated P3HT/GaAs hybrid solar cells. The contribution of P3HT¹⁵ is visible in the left tail of the EQE plot, showing that absorption of light by the

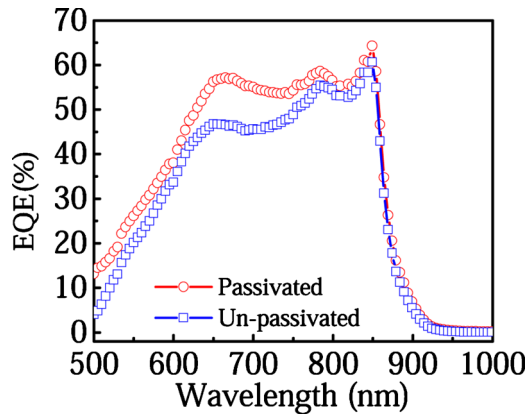


FIG. 5. (Color online) External quantum efficiency measurements of passivated and unpassivated hybrid solar cells.

polymer (with absorption coefficient $\sim 3 \times 10^5 \text{ cm}^{-1}$ @ $\lambda = 500 \text{ nm}$) contributes to the photocurrent, despite the fact that the P3HT film is quite thin. Moreover, the absorption of GaAs is also apparent throughout the entire EQE spectrum, showing that the hybrid device also has a significant fraction of photocurrent that results from absorption in GaAs and subsequent hole transfer to P3HT. The fact that absorption from both components contributes to the photocurrent provides a match with the solar spectrum that would be difficult to achieve with either component alone. Figure 5 also shows that surface passivation of the nanopillars increases the EQE across the entire absorption range; this indicates improved carrier collection, which most likely results from reduced trapping and/or recombination that occurs at surface defects on the GaAs nanopillars.

In summary, we report a hybrid solar cell that combines *n*-doped GaAs nanopillars grown by catalyst-free MOCVD deposition and P3HT, a *p*-type semiconducting polymer. The PV device shows a promising power conversion efficiency of $\eta = 0.6\%$. Ammonium sulfide passivation improves the chemical and electronic properties of the nanostructure surface, resulting in an improved solar cell efficiency of η

$= 1.44\%$. A systematic and methodical study of these hybrid polymer/inorganic semiconductor interfaces will be crucial for the optimization of photon absorption, carrier collection/extraction and other phenomena that currently limit the overall power conversion efficiency of solar cells.

The authors thank the financial support of this research by NSF (Grant Nos. ECCS-0824273 and CHE-0527015), DoD (Grant No. NSSEFF N00244-09-1-0091), ONR (Contract No. N00014-04-1-0410), and NSF IGERT (Contract No. 0903720). This work was performed, in part, at the Center for Integrated Nanotechnologies, an U.S. Department of Energy, Office of Basic Energy Sciences user facility at Los Alamos National Laboratory (Contract DE-AC52-06NA25396) and Sandia National Laboratories (Contract No. DE-Ac04-94AL85000).

- ¹L. Chen, Z. Hong, G. Li, and Y. Yang, *Adv. Mater. (Weinheim, Ger.)* **21**, 1434 (2009).
- ²M. A. Green, K. Emery, Y. Hishikawa, and W. Warta, *Prog. Photovoltaics*, **18**, 144 (2010).
- ³C. Y. Liu, C. Zachary, U. Holman, and R. Kortshagen, *Nano Lett.* **9**, 449 (2009).
- ⁴W. U. Huynh, J. J. Dittmer, and A. P. Alivisatos, *Science* **295**, 2425 (2002).
- ⁵R. Plass, S. Pelet, J. Krueger, and M. Grätzel, *J. Phys. Chem. B* **106**, 7578 (2002).
- ⁶H. Bi and R. R. LaPierre, *Nanotechnology* **20**, 465205 (2009).
- ⁷J. L. Pau, C. Bayram, P. Giedraitis, R. McClintock, and M. Razeghi, *Appl. Phys. Lett.* **93**, 221104 (2008).
- ⁸G. R. Lin, Y. C. Chang, E. S. Liu, H. C. Kuo, and H. S. Lin, *Appl. Phys. Lett.* **90**, 181923 (2007).
- ⁹K. Ikejiri, J. Noborisaka, S. Hara, J. Motohisa, and T. Fukui, *J. Cryst. Growth* **298**, 616 (2007).
- ¹⁰V. Schmidt, S. Senz, and U. Gösele, *Appl. Phys. A: Mater. Sci. Process.* **86**, 187 (2006).
- ¹¹M. T. Björk, H. Schmid, J. Knoch, H. Riel, and W. Riess, *Nat. Nanotechnol.* **4**, 103 (2009).
- ¹²M. V. Lebedev, *Prog. Surf. Sci.* **70**, 153 (2002).
- ¹³T. Ohno, *Surf. Sci.* **255**, 229 (1991).
- ¹⁴H. Oigawa, J. F. Fan, Y. Nannichi, H. Sugahara, and M. Oshima, *Jpn. J. Appl. Phys., Part 2* **30**, L322 (1991).
- ¹⁵V. Shrotriya, J. Ouyang, R. J. Tseng, G. Li, and Y. Yang, *Chem. Phys. Lett.* **411**, 138 (2005).